Non-linear precoding for 5G NR

Fumihiro Hasegawa, Hiroshi Nishimoto,
Akinori Taira, Akihiro Okazaki, Atsushi Okamura
Mitsubishi Electric Corporation
Information Technology R&D Center
5-1-1 Ofuna, Kamakura, Kanagawa, 247-8501, Japan
Hasegawa.Fumihiro@bk.mitsubishielectric.co.jp

Nuan Song †, Mihail Enescu ‡
† Nokia Shanghai Bell
388#, Ningqiao Road, Jinqiao Pudong,
Shanghai, P. R. China
‡ Nokia Solutions and Networks
Karaportti 7, Espoo, Finland
nuan.song@nokia-sbell.com

***Abstract*—Non-linear precoding gained attention recently in 3GPP (the third generation partnership project) as a possible technique to improve the performance of multi-user multiple input multiple output (MIMO). In this paper, research and standardization activities related non-linear precoding for 3GPP are described. Implementation, performance evaluation of nonlinear precoding and analysis of 3GPP specification impact are presented in this paper. Both system and UE throughput evaluation results, conducted at both 5GHz and 30GHz, demonstrate that non-linear precoding yield superior performance compared to linear precoding. In addition, two novel non-linear precoding based transmission schemes which require lower computational complexities than conventional non-linear precoding schemes are proposed. The first scheme separates UEs into linearly precoded and nonlinearly precoded UEs, reducing computational complexities required by non-linear precoding. The second scheme is a precoding scheme which intentionally introduces inter-UE interference through linear precoding and implements non-linear precoding to remove inter-UE interference; multi-user diversity gain and reduction in computational complexity are obtained simultaneously. Finally, new abstraction performance metrics for the proposed schemes are presented. The simulation results demonstrate that the proposed methods outperform linear precoding techniques and offer a tradeoff between computational complexity and throughput performance.**

***Index Terms*—Non-linear precoding, 3GPP, 5G, NR**

I. Introduction

MIMO transmission has gained considerable attention recently due to its potential to increase the system throughput dramatically [1]. In the 5G NR (New Radio) interface specification approved in June 2018, multiple antenna techniques are included to improve spectral efficiency and coverage for sub and over 6GHz spectrum, respectively [2]. For multi-user multiple input multiple output (MU-MIMO), linear precoding (LP) is a conventional approach to separate users spatially. Among various approaches in LP, block diagonalization (BD) is a well-known technique to create prescribed nulls for user equipment (UE) except for the target UE in order to mitigate inter-user interference (IUI) [3]. BD precoding is effective in a spatially-uncorrelated scenario and simplifies receiver designs. However, by consuming degrees of freedoms in MIMO systems to create perfect nulls for non-target UEs, a tradeoff between interference mitigation and achievable spatial diversity arises. Moreover, IUI mitigation performance of LP degrades considerably in ill-conditioned or spatially-correlated channels, limiting achievable throughput. Such channels can be found in crowded environment where channels seen by UEs may overlap spatially.

With full channel state information (CSI) at the transmitter side, a non-linear precoding (NLP) technique such asDirty-Paper Coding (DPC) that relies on a pre-subtraction of the non-causally known interference can achieve the maximum sum rate of the system and provide the maximum diversity order [4]. Tomlinson-Harashima Precoding (THP) [5], [6] is a simplified and efficient version of DPC, which is less computationally demanding and thus more attractive for practical implementation. NLP such as THP is able to provide a significantly enhanced system performance as compared to LP such as BD [7], especially for correlated channels where the subspaces of UEs are overlapped.

However, there are several technical challenges to implement NLP.

- Large array: In NR MIMO systems, both the base station and UEs are mounted with more antennas than those in LTE systems, especially at the base station side, where a large antenna array is usually applied. This may lead to a prohibitively high complexity and overwhelming overhead to implement NLP.
- Receive demodulation: When UE has multiple antennas and the number of antennas is usually larger than the number of data streams, receive combining at the UE side that maps from antennas to streams is required. NLP leads to different reception procedures at UEs.
- CSI sensitivity: NLP is more sensitive to CSI errors than LP, since linear precoding is based on the spatial signal subspace calculations, whereas THP precoding is a non-causal interference pre-subtraction scheme.

While a considerable amount of standardization work related to 5G MIMO is being conducted in 3GPP [8], [9], outcome of discussions on NLP in 3GPP considering the previously described challenges in various 3GPP 5G scenarios is summarized in [10]. In this paper, research and standardization activities related NLP for 3GPP are described. Furthermore, solutions to reduce computational complexity of NLP are introduced. Finally, impact of NLP on the 3GPP specification and performance evaluation results of the proposed schemes considering CSI error are shown in this paper.

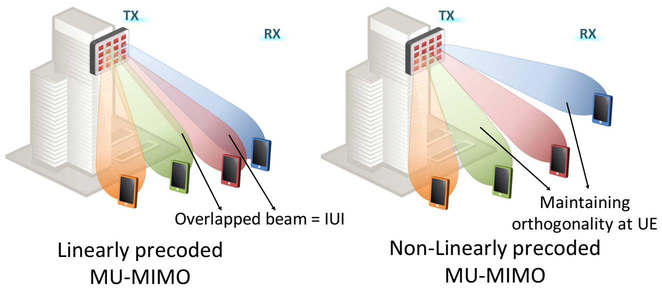

Fig. 1: Illustrative comparison of linear and NLP

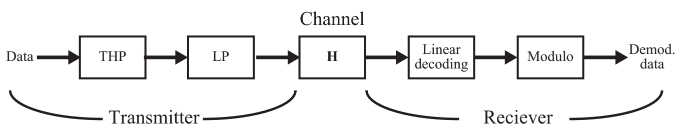

Fig. 2: Block diagram of transmitter with THP based non-linear precoder and receiver

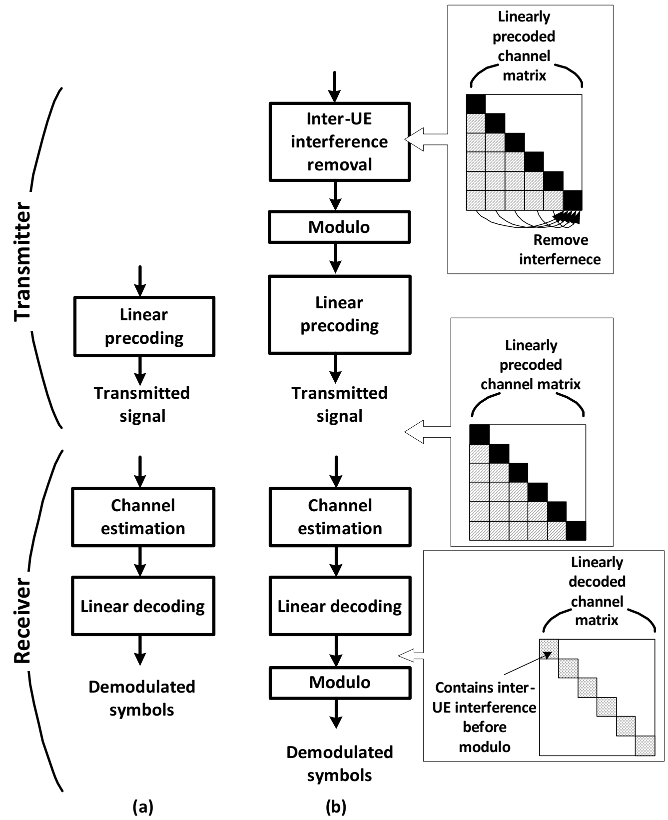

Fig. 3: Comparison of data processing at both transmitter and receiver for (a) linear precoding and (b) block triangulation

II. Non-linear Precoding and Linear Precoding

Let us introduce a $N_{\mathrm{Rx},i} \times N_{\mathrm{Tx}}$ channel matrix $\mathbf{H}_i$ capturing channel coefficients between i^{th} UE and transmitter, where $N_{\mathrm{Rx},i}$ and N_{Tx} denote the number of receive antennas for the i^{th} UE and transmit antennas at the base station, respectively. We also denote the total number of receive antennas as $N_{\mathrm{R}x} = \sum_{i=1}^{K} N_{\mathrm{Rx},i}$.

We assume that there are K UEs in the system and $1 \leq N_{\mathrm{st},i} \leq N_{\mathrm{Rx},i}$, $N_{\mathrm{Rx}} \leq N_{Tx}$, where $N_{\mathrm{st},i}$ is the number of data streams transmitted to the i^{th} UE. If we denote $N_{\mathrm{Tx}} \times N_{\mathrm{st},i}$ $\mathbf{B}_i$ as the precoding matrix for the i^{th} UEs symbols, the precoded channel matrix can be written as follows,

$$\begin{bmatrix} \mathbf{H}_1\mathbf{B}_1 & \mathbf{H}_1\mathbf{B}_2 & \cdots & \mathbf{H}_1\mathbf{B}_K \\ \mathbf{H}_2\mathbf{B}_1 & \mathbf{H}_2\mathbf{B}_2 & \cdots & \mathbf{H}_2\mathbf{B}_K \\ \vdots & \vdots & \ddots & \vdots \\ \mathbf{H}_K\mathbf{B}_1 & \mathbf{H}_K\mathbf{B}_2 & \cdots & \mathbf{H}_K\mathbf{B}_K \end{bmatrix}. \tag{1}$$

In conventional precoder designs, the LP matrices should be designed such that null beams are created for unintended UEs. Thus, the desired channels after precoding can be written as follows

$$\begin{bmatrix} \mathbf{H}_1\mathbf{B}_{\mathrm{BD},1} & 0 & \cdots & 0 \\ 0 & \mathbf{H}_2\mathbf{B}_{\mathrm{BD},2} & \cdots & 0 \\ \vdots & \vdots & \ddots & \vdots \\ 0 & 0 & \cdots & \mathbf{H}_K\mathbf{B}_{\mathrm{BD},K} \end{bmatrix}, \tag{2}$$

where the i^{th} UE does not experience any interfering beams from other UEs.

NLPis used to cancel IUI, simultaneously obtaining multi-user diversity and received signal which is free of IUI. The following example demonstrates how LP can be used to introduce intentional interference to obtain MU diversity and use NLP to resolve IUI. In the first step, LP matrix is designed, or other known block triangulation (BT) techniques are implemented, such that $\mathbf{H}_i\mathbf{B}_j = 0$ for $i < j$, which produces the following channel matrix,

$$\begin{bmatrix} \mathbf{H}_1\mathbf{B}_{\mathrm{BT},1} & 0 & \cdots & 0 \\ \mathbf{H}_2\mathbf{B}_{\mathrm{BT},1} & \mathbf{H}_2\mathbf{B}_{\mathrm{BT},2} & \cdots & 0 \\ \vdots & \vdots & \ddots & \vdots \\ \mathbf{H}_K\mathbf{B}_{\mathrm{BT},1} & \mathbf{H}_K\mathbf{B}_{\mathrm{BT},2} & \cdots & \mathbf{H}_K\mathbf{B}_{\mathrm{BT},K} \end{bmatrix}. \tag{3}$$

In the second step, the remaining IUI due to the non-diagonal blocks in (3) is cancelled at the transmitter by applying NLP using a feedback filter. An illustrative comparison between LP and NLP is shown in Figure 1. An example of a block diagram of NLP based transmitter and receiver is shown in Figure 2. A flowchart illustrating data processing at both transmitter and receiver is shown in Figure 3. For BT, non-linear precoding is implemented at the transmitter to perform pre-cancelation of inter-UE interference. Pre-cancellation of inteference leads to increase in peak to average power ratio (PAPR). Thus, modulo operation is implemented to maintain PAPR at a reasonable level. At the receiver side, UE performs modulo operation to demodulate data symbols.

To illustrate and compare obtained signal to interference noise ratio (SINR) between LP and NLP, heat maps are shown in Figure 4. In Figure 4, eight UEs are placed in front of the base station while one of the UEs is the target UE. Difference

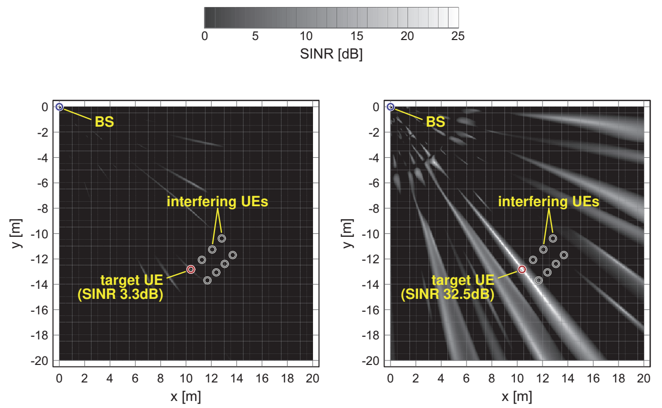

(a) Block diagonal precoding (b) BT with THP

Fig. 4: Comparison of SINR heat map between block diagonal precoding and block triangular precoding with THP

in the effect of precoding between LP and NLP is illustrated by showing the acquired SINR map. From the figure, it is clear that SINR at the target UE is higher for NLP, demonstrating its ability to isolate the target UE and reduce IUI.

III. 3GPP Specification Impact

NLP requires specific receive procedures at UEs. As usually mounted with multiple antennas, UEs should carry out receive combining before weighting and demodulating non-linearly precoded data. We propose two modes for the UE reception procedure to implement receive combining. Such receive combining is designed independent of or dependent on the NLP procedure, according to the beamformed CSI or the full downlink CSI. The latter can be applied to achieve a performance enhancement.

To acquire full downlink CSI in the 3GPP framework, sounding reference signal (SRS) supported in NR can be used in reciprocity based CSI acquisition in TDD. In addition, Type-II based CSI feedback using codebooks with higher resolution or analog feedback can also be considered for CSI feedback methods for NLP. NLP requires accurate CSI to achieve perfect interference cancellation at the transmitter. Thus, a mechanism such as the aforementioned techniques for the transmitter to acquire accurate CSI in a timely manner is needed.

NLP or LP can be switched dynamically or used jointly with LP. Since the modulo operation is needed at the receiver for optimal demodulation of NLP signals, the transmitter needs to signal precoding type to UE. In terms of reference signals, demodulation reference signal (DMRS), defined in 3GPP specification to estimate channels during demodulation, need to be designed for NLP. For linearly precoded systems, UEs can estimate fading channels combined with precoding matrices since precoding matrices are transparent to UEs. Moreover, interference from other UEs can be estimated using DMRS assigned to different UEs. Using nonlinearly precoded signals, estimation of the channel or interference is not straightforward. Thus, treatment of DMRS for NLP requires careful inspection.

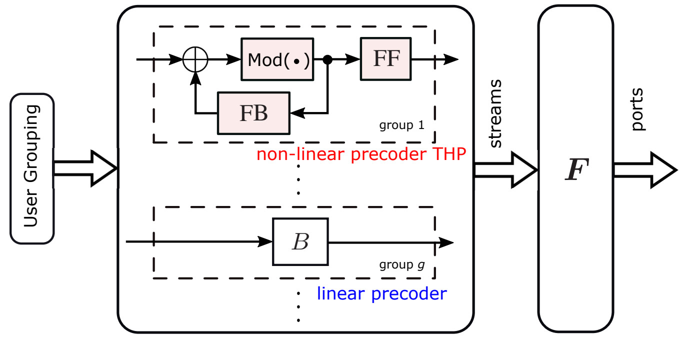

Fig. 5: Block diagram of the proposed advanced NLP scheme.

One solution is to use LP and NLP for DMRS and data transmission, respectively.

IV. Advanced Non-linear Precoding Techniques

A. Reduced rank precoding

Firstly, a novel precoding scheme which splits UEs into linearly precoded UEs and non-linearly precoded UEs is described here. In NR networks, there will be various types of UEs, where some UEs are legacy ones and some are NLP capable UEs. The base station should be able to accommodate different UEs and carry out advanced precoding techniques for a performance enhancement. To improve the system as well as UE's performance and meanwhile to alleviate the complexity for large-scale antenna systems, we propose a reduced-rank precoding technique as described in Figure 5. It is assumed that the scheduled users are divided into several groups. The whole precoding procedure consists of two stages. The outer LP acts like a low-rank transformation, mapping from antenna elements at the base station of a dimension N_{Tx} to the sum of the antenna elements at each UE group. It aims at mitigating inter-group interference (or decoupling), which can be designed based on the long-term CSI, for example, using the BD or Signal-to-Leakage-and-Interference Ratio (SLNR) algorithm. Alternatively, the outer processing can also be implemented by analog beamforming, where each analog beam is directed to the corresponding group of users and those beams are kept as separated as possible. The inner precoding is carried out in a reduced dimension in parallel for groups, where either LP or NLP can be applied to effectively suppress the IUI within each group.

This proposal supports both linear and NLPfor various UEs simultaneously as well as dynamic changes of precoding types for UEs at different occasions. Figure 6 shows one example of a communication network including both LP and NLP for various types of UEs. It is a single-cell scenario, where one base station serves 8 UEs simultaneously. At time t, UEs marked with numbers 1 - 5 that form the group 1 are linearly precoded and UEs with 6 - 8 in group 2 are non-linearly precoded. At time $t + \Delta t$, UE 5 moves and gets closer to the UEs in group 2, indicating a worse channel condition. The base station tries to improve UE 5's performance by NLP.

The proposed precoding technique allows the base station to dynamically update its precoding by re-decoupling of UE groups and to perform precoding for each group.

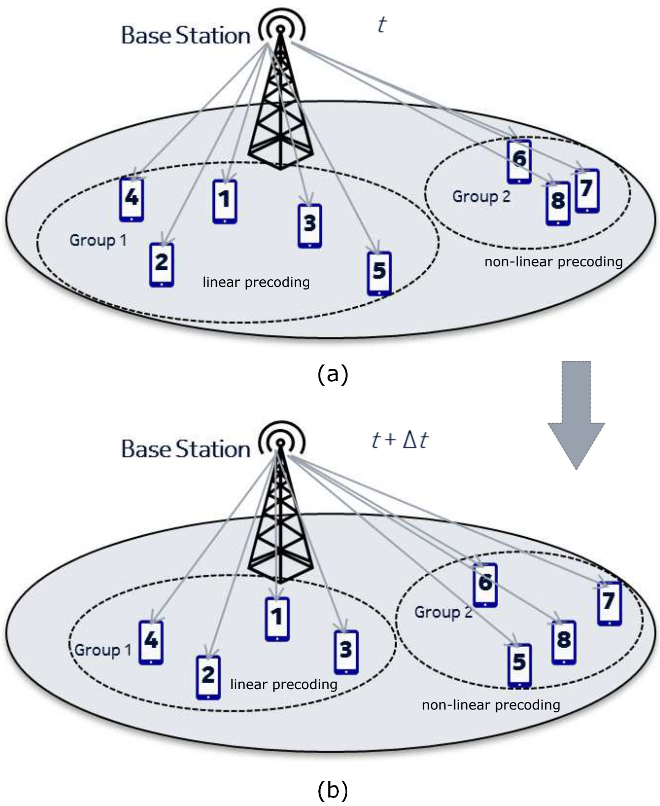

Fig. 6: One example of a communication network including both LP and NLP for two groups of UEs.

B. Block multiple diagonal precoding

The proposed precoding scheme which yields multi-user diversity at low computational complexity is described in this subsection. The aim is to introduce correlation among several UEs in a group and implement NLP to eliminate inter UE interference while maintaining low computational complexity. Computational complexity required for interference cancellation is proportional to the number of off-diagonal matrices in the equivalent channel matrix. Assuming K is an even number, it is clear that from (3) and (4) that there are $\frac{K(K-1)}{2}$ and $K-1$ off-diagonal matrices, respectively. Thus, computational complexity can be reduced by $K/2$ fold. Through grouping, spatial diversity gain can be obtained. In the proposed method, namely block multiple diagonal (BMD) precoding, UEs are grouped such that NLP is performed within the group. Let us denote $\mathbf{B}_i'$ and G_S as the BMD precoding matrix for the i^{th} UE and number of UEs in a group, respectively. In this paper, it is assumed that all groups contain the same number of UEs. Then, the precoded matrix can be characterized as $\mathbf{H}_i\mathbf{B}_j' = 0$ for $i < j$ and for $i \geq j + G_S$. Detailed procedure to generate precoding matrices is described in [11]. As an example, the precoded channel matrix with a pair of UEs in a group, $G_S = 2$, can be written as follows,

$$\begin{bmatrix} \mathbf{H}_1\mathbf{B}_1' & 0 & \cdots & 0 & 0 \\ \mathbf{H}_2\mathbf{B}_1' & \mathbf{H}_2\mathbf{B}_2' & \cdots & 0 & 0 \\ 0 & \mathbf{H}_3\mathbf{B}_2' & \cdots & 0 & 0 \\ \vdots & \vdots & \ddots & \vdots & 0 \\ 0 & 0 & \cdots & \mathbf{H}_K\mathbf{B}_{K-1}' & \mathbf{H}_K\mathbf{B}_K' \end{bmatrix}. \tag{4}$$

It should be noted that assignment of UEs to groups depends on scheduling and UEs are grouped according to the distance between each other; UEs who are located in the similar Azimuth direction with respect to the base station are grouped together.

V. Evaluation Methodologies: System Level Evaluation in the Presence of CSI Imperfections

System level evaluations consider system parameters such as scheduling algorithms, traffic pattern and locations of UEs with respect to the base station [12]. To analyze system level performance of MU-MIMO schemes, system level simulations must be conducted. To expedite evaluation, one approach to characterize link-level performance of a scheme is to abstract link-level performance so that a look up table, which associates SINR and a performance metric, can be used to assess the performance. In the following, examples of abstraction metrics which incorporate CSI estimation error for LP, NLP and hybrid method are described.

A simple but accurate error model for channel estimations is required to evaluate NLP schemes. The model that allows expressing the channel estimation error as SINR degradation or as an additional noise term can be considered. The performance of an estimator is approximated by modelling the channel estimation error as a modified Gaussian noise. The erroneous channel can be written as $\boldsymbol{H}_{err} = \boldsymbol{H} + \Delta\boldsymbol{H}$, where $\Delta\boldsymbol{H}$ is the channel estimation error added to the perfect CSI $\boldsymbol{H}$. The precoding matrix $\boldsymbol{B}$ is designed based on $\boldsymbol{H}_{err}$ and the resulting effective channel can be written as $\boldsymbol{H}\boldsymbol{B} = \boldsymbol{H}_{err}\boldsymbol{B} - \Delta\boldsymbol{H}\boldsymbol{B}$. For LP such as BD, the first term has a block diagonal structure and the error term $\Delta\boldsymbol{H}\boldsymbol{B}$ causes non-zeros at off-diagonal entries. If we represent the effective channel after decoding as $\hat{\boldsymbol{H}}$, assuming the equal power allocation is used for transmission, the received SINR for the l-th data stream can be approximated by

$$\mathrm{SINR}_l \approx \frac{\frac{P_T}{r}\left|\hat{\boldsymbol{H}}(l,l)\right|^2}{\sigma_n^2 + \frac{P_T}{r}\sum_{i=1,i\neq l}^{r}\left|\hat{\boldsymbol{H}}(l,i)\right|^2} \tag{5}$$

where r, P_T and σ^2 are the total number of data streams, transmission power and the noise covariance respectively. The interference term in the denominator occurs in the presence of channel imperfections.

For NLP with BT, by assuming that the statistics of signals at the output of the feedback structure approximate those of the original data except for a power loss, a similar SINR calculation as that for LP can be derived. Given that the feedforward filter of THP is also denoted by $\boldsymbol{B} =$

$\left[\begin{array}{cccc} \boldsymbol{B}_1 & \boldsymbol{B}_2 & \dots & \boldsymbol{B}_K \end{array}\right] \in \mathbb{C}^{N_{\mathrm{Tx}} \times N_{\mathrm{Rx}}}$ based on the channel matrix $\boldsymbol{H} = \left[\begin{array}{cccc} \boldsymbol{H}_1^T & \boldsymbol{H}_2^T & \dots & \boldsymbol{H}_K^T \end{array}\right]^T \in \mathbb{C}^{N_{\mathrm{Rx}} \times N_{\mathrm{Tx}}}$, the total effective channel before receive processing $\tilde{\boldsymbol{H}} = \boldsymbol{H}\boldsymbol{B}$ becomes lower triangular as shown in (3), where the upper triangular entries turn out to be zeros, i.e., $\boldsymbol{H}_i\boldsymbol{B}_j = \boldsymbol{0}, \quad j > i$, in the ideal case. Based on the effective channel $\tilde{\boldsymbol{H}}$ and the equivalent residual error term from the interference $\Delta\tilde{\boldsymbol{H}}$ after weighting at the receiver, the SINR for the l-th data stream is computed by

$$\mathrm{SINR}_l = \frac{\frac{P_T}{r}\left|\tilde{\boldsymbol{H}}(l,l)\right|^2}{\sigma_n^2 + \frac{P_T}{r}\sum_{i=l+1}^{r}\left|\tilde{\boldsymbol{H}}(l,i)\right|^2 + \frac{P_T}{r}\sum_{i=1}^{l-1}\left|\Delta\tilde{\boldsymbol{H}}(l,i)\right|^2}, \tag{6}$$

where interference term occurs when channel imperfections are present. For NLP with BMD, the following approach can be taken to obtain the abstraction metric. Let us assume that all UEs receive the same number of streams, i.e., $N_{st} = N_{st,i}$ $\forall i$. Then, the SINR expression for the i^{th} UE can be write as follows,

$$\mathrm{SINR}_l = \frac{\frac{P_T}{r}\left|\tilde{\boldsymbol{H}}(l,l)\right|^2}{\sigma_n^2 + \frac{P_T}{r}\left(\alpha_l + \sum_{i=1}^{l-1}\left|\Delta\tilde{\boldsymbol{H}}(l,i)\right|^2\right)}, \tag{7}$$

with $\alpha_l = \sum_{i=l+1}^{l+G_{st}-1}\left|\tilde{\boldsymbol{H}}(l,i)\right|^2 + \sum_{i=l+G_{st}}^{r}\left|\Delta\tilde{\boldsymbol{H}}(l,i)\right|^2$ and $G_{st} = G_S N_{st}$. By observing α_l, inter-stream interference and IUI from UEs outside of the group contribute to degradation in performance.

VI. Evaluation Results: Link Level Simulation Results

In this section, simulation results are presented to compare performance of the proposed methods against conventional methods. Performance evaluation is conducted at 5GHz and 30GHz, reflecting “FR1” an “FR2” spectrums defined for NR [2]. Firstly, we evaluate the cell throughput and UE throughput performance of various precoding schemes for 5GHz. The terms ’BD’ and ’THP’ correspond to the cases when all the UEs are either linearly or non-linearly precoded, respectively. The proposed hybrid technique is referred to as ’THP-BD’. In the experiment we consider two groups of UEs denoted by (X, Y), where one with X UEs uses LP and the other one with Y UEs applies NLP. We apply the local area small office scenario defined in the WINNER II channel model [13], where the base station is mounted with 16 antennas and in total 8 UEs, each with 2 antennas. Detailed simulation parameters can be found in Table I. In the table, “chunk size” refers to the duration in both time and frequency during which the same precoding matrix is used. For 30 GHz simulation, clustered delayed model (CDL)-D defined in [14] is implemented. The channel model is modeled based on indoor hotspot environment and characterized by its strong line of sight (LoS) component.

TABLE I: Simulation Setup

Carrier frequency	5 GHz	30 GHz
Channel model	WINNER II Local area small office scenario[13]	CDL-D [14]
Bandwidth	89 MHz	95MHz
Chunk size	8 subcarriers 15 OFDM symbols	12 subcarriers 14 OFDM symbols
Antennas at base station	16 ULA	16 subarrays 64 elements/subarray
Antennas at UEs	2 ULA	Bipolar antenna
UE velocity	3 km/h	{0, 3} km/h

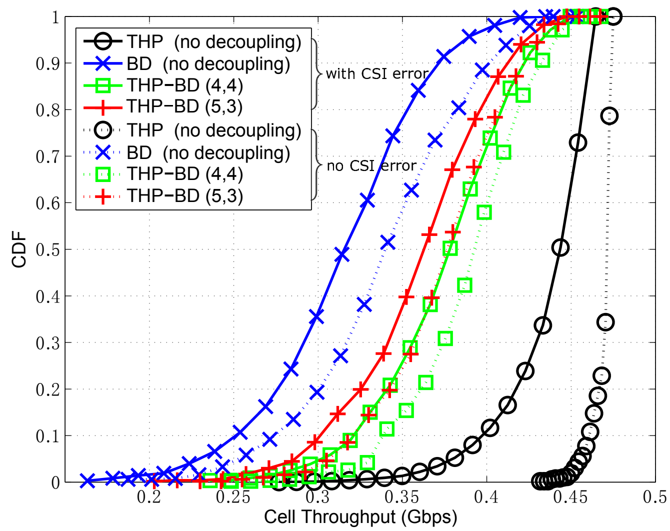

Fig. 7: CDF of the cell throughput performance of the proposed technique with and without CSI error.

Figures 7 and 8 depict the cumulative distribution function (CDF) of the cell throughput as well as the UE throughput for different precoding schemes with and without CSI error. From Figure 7 we can observe that the ’THP’ scheme provides the best performance under the perfect CSI condition for all UEs, while a large performance degradation is observed in the presence of CSI error especially for the cell-edge UEs. The ’BD’ precoding method is also affected by the CSI error, but is not that sensitive as compared to THP. The performance of the proposed ’THP-BD’ scheme lies between that of the standard BD and THP methods. We consider two cases, where one corresponds to (5,3) and the other is (4,4), indicating that for the latter one UE has changed its precoding type from ’BD’ to ’THP’, as depicted in the scenario Figure 6. It is obvious that the cell throughput performance improves if more UEs are non-linearly precoded. The performance of individual UEs in the presence of CSI error is also shown in Figure 8. It can be observed that if all the UEs are non-linearly precoded by ’THP’, good performance can be achieved but at the expense of a high system complexity. The UE’s performance does not vary much for different UE conditions if LP ’BD’ is used. For the proposed scheme, the UE who has changes its precoding type (with the star marker) obtains a great performance enhancement.

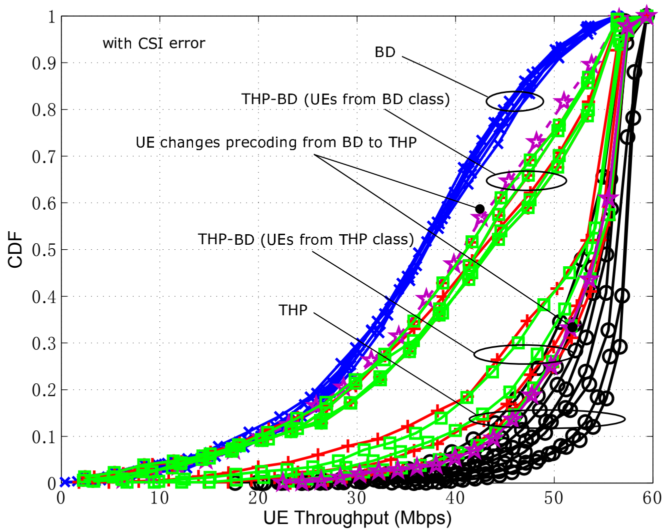

Fig. 8: CDF of the UE throughput performance of the proposed technique with CSI error.

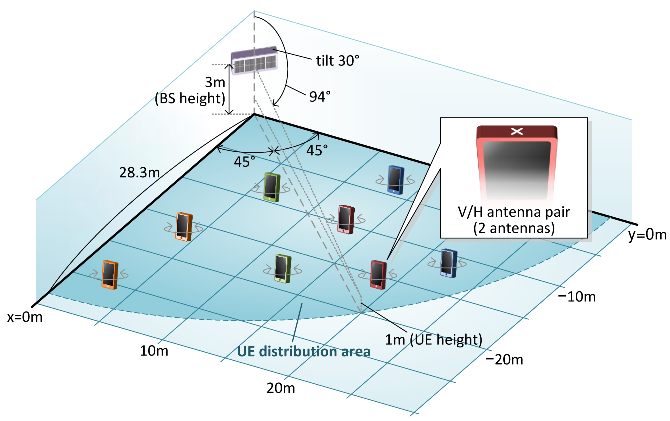

Fig. 9: Location of UEs and base station for 30GHz evaluation

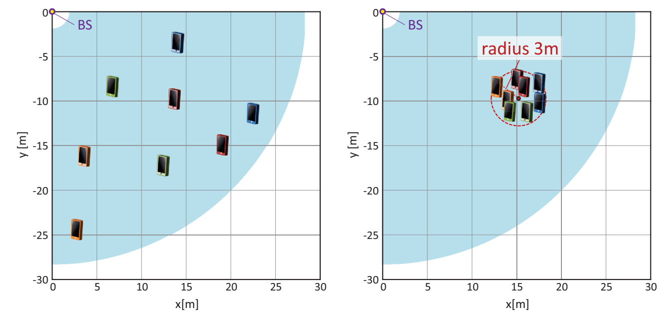

(a) sparse (b) dense

Fig. 10: Dense and sparse UE placement for 30GHz evaluation

In the following, throughput evaluation assumptions and evaluation results for 30GHz are shown. The evaluation parameters are shown in Table I. Due to sensitivity of UE locations and height of base station on simulation results at 30GHz, detailed parameters of the simulated environment are illustrated in Figure 9. In addition, performance of LP and NLP are evaluated with two different densities of UEs. Both dense and sparse UE densities, illustrated in Figure 10, are used in the evaluation. CDF of the cell and UE throughput are shown in Figure 11 and 12, respectively. The performance curve labeled "BMD" indicates the performance of BMD when NLP is implemented to cancel IUI among the grouped UEs. The performance curve labeled "THP-BD (4,4)" indicates the performance of the hybrid scheme in which 8 UEs are split into two groups and THP and BD are implemented separately. A random scheduling algorithm was implemented to separate UEs into two groups. From the figures, it is clear that THP yields the best throughput performance compared to BD or BMD. Thanks to the diversity gain obtained from grouping UEs and use of THP, BMD yields better performance compared to BD. It is also noticeable that the performance gap between BMD and hybrid scheme is small. It is also clear from the figures that CSI error degrade performance of both LP and NLP based methods. Finally, effect of density of UEs is evaluated in the simulation. In the sparse condition, due to insignificant amount of IUI, better throughput performance can be obtained for all schemes. It is also noticeable that the performance difference among various methods is small. In the dense environment, due to severe IUI among UEs, throughput performance degrades. However, using THP, BMD or hybrid method, IUI can be removed and throughput performance can be improved, compared to BD.

Finally, tradeoff between computational complexity and system throughput performance is illustrated in Figure 13 for CDF=20% and CDF=90%. Computational complexity is estimated by the number of off-diagonal matrices in the precoded channel matrix. The system throughput in Figure 13 is obtained when UEs are stationary and placement of UE is dense, as illustrated in Figure 10. In addition, it is assumed that ideal channel estimates are available at UEs. It is clear from the figure that while the best throughput performance can be obtained by THP at the expense of complexity, both hybrid method and BMD offer tradeoff between computational complexity and system throughput.

VII. Conclusion

Performance evaluations of various NLP schemes and effect of channel estimation error are investigated in this paper. NLP schemes with lower computational complexity are proposed and performance metrics that can be used for abstraction for system level simulations are introduced in the paper. In addition, specification impacts created by NLP on 3GPP specifications are explained. From the evaluation results, NLP based method yield better performance at both 5GHz and 30GHz. Moreover, the proposed methods, which offer a tradeoff between performance and computational complexity, yield comparable throughput performance to THP schemes. The proposed techniques combined with rate splitting techniques [15] can be investigated in the future for further per-

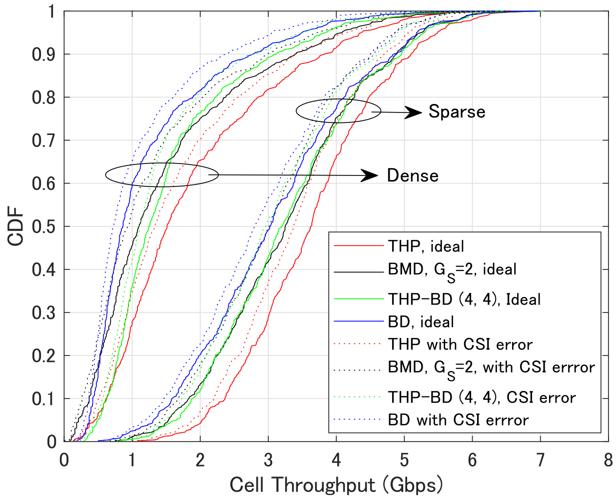

Fig. 11: CDF of the cell throughput of BD, THP, BMD and hybrid scheme with and without CSI error for different UE densities at 30GHz

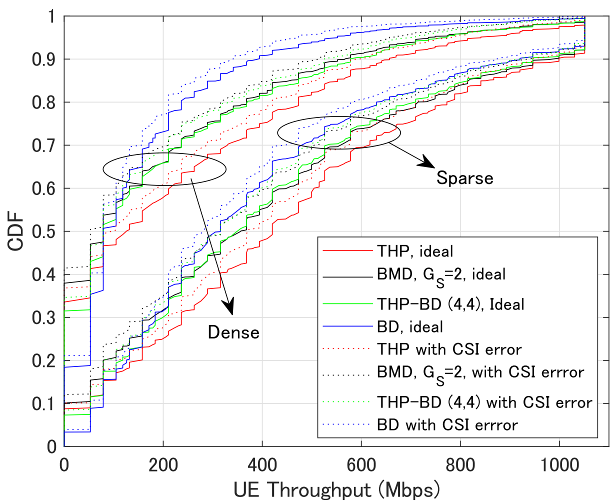

Fig. 12: CDF of the UE throughput of BD, THP, BMD and hybrid scheme with and without CSI error for different UE densities at 30GHz

formance improvement. The technical proposals, SINR based metric for system level performance evaluation and discussions on specification impact in 3GPP presented in this paper will hopefully motivate investigations of applicability of NLP for 5G NR and create new areas for technical proposals.

VIII. Acknowledgment

The work conducted by Mitsubishi Electric includes a part of the results of “The research and development project for realization of the fifth-generation mobile communications system” commissioned by Japan’s Ministry of Internal Affairs and Communications.

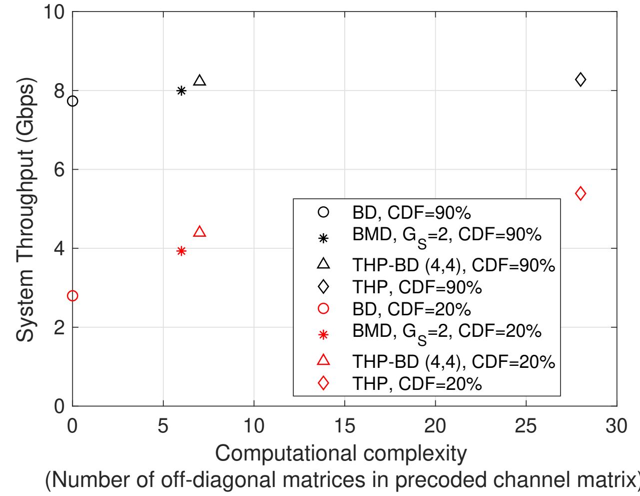

Fig. 13: Tradeoff between computational complexity and system throughput

References

[1] E. G. Larsson, O. Edfors, F. Tufvesson, and T. L. Marzetta, “Massive MIMO for next generation wireless systems,” *IEEE Communications Magazine*, vol. 52, no. 2, pp. 186–195, February 2014.

[2] B. Bertenyi, S. Nagata, H. Kooropaty, X. Zhou, W. Chen, Y. Kim, X. Dai, and X. Xu, “5G NR Radio Interface,” *Journal of ICT Standardization*, vol. 6, pp. 31–58, May 2018.

[3] R. Rajashekar and L. Hanzo, “Iterative Matrix Decomposition Aided Block Diagonalization for mm-Wave Multiuser MIMO Systems,” *IEEE Transactions on Wireless Communications*, vol. 16, no. 3, pp. 1372–1384, March 2017.

[4] M. Costa, “Writing on dirty paper,” *IEEE transactions on information theory*, vol. 29, no. 3, pp. 439–441, 1983.

[5] M. Tomlinson, “New automatic equaliser employing modulo arithmetic,” *Electronics letters*, vol. 7, no. 5, pp. 138–139, 1971.

[6] H. Harashima and H. Miyakawa, “Matched-transmission technique for channels with intersymbol interference,” *IEEE Transactions on Communications*, vol. 20, no. 4, pp. 774–780, 1972.

[7] Q. H. Spencer, A. L. Swindlehurstand, and M. Haardt, “Zero-forcing methods for downlink spatial multiplexing in multiuser MIMO channels,” *IEEE Transactions on Signal Processing*, vol. 52, no. 2, pp. 461–471, 2004.

[8] S. Parkvall, E. Dahlman, A. Furuskar, and M. Frenne, “NR: The New 5G Radio Access Technology,” *IEEE Communications Standards Magazine*, vol. 1, no. 4, pp. 24–30, Dec 2017.

[9] E. Onggosanusi, M. S. Rahman, L. Guo, Y. Kwak, H. Noh, Y. Kim, S. Faxer, M. Harrison, M. Frenne, S. Grant, R. Chen, R. Tamrakar, and Q. Gao, “Modular and High-Resolution Channel State Information and Beam Management for 5G New Radio,” *IEEE Communications Magazine*, vol. 56, no. 3, pp. 48–55, MARCH 2018.

[10] “WF on analysis of nonlinear precoding,” 3GPP, R1-1704009, Feb. 2017.

[11] H. Nishimoto, A. Taira, H. Iura, S. Uchida, A. Okazaki, and A. Okamura, “Performance evaluation of NL-BMD precoding over analog-digital hybrid beamforming for High SHF wide-band massive MIMO in 5G,” *Int. J. Wireless Inf. Networks*, vol. 24, no. 3, pp. 225–239, 2017.

[12] L. Chenand, W. Chen, B. Wang, X. Zhang, H. Chen, and D. Yang, “System-level simulation methodology and platform for mobile cellular systems,” *IEEE Communications Magazine*, vol. 49, no. 7, pp. 148–155, JULY 2011.

[13] WINNER, “Test Scenarios and Calibration Cases Issue 2,” IST-4-027756 WINNER II, D6.13.7 v1.00, July 2007.

[14] 3GPP, “Study on Channel Model for Frequency Spectrum Above 6 GHz,” *TR 38.900, V14.3.1*, Jul. 2017.

[15] M. Dai, B. Clerckx, D. Gesbert, and G. Caire, “A rate splitting strategy for massive mimo with imperfect csit,” *IEEE Transactions on Wireless Communications*, vol. 15, no. 7, pp. 4611–4624, July 2016.